The Cerebellum Shrinks Faster Than Normal Ageing in Alzheimer's Disease but not in Mild Cognitive Impairment

Hossein Tabatabaei-Jafari,* Erin Walsh, Marnie E. Shaw, and Nicolas Cherbuin, for the Alzheimer's Disease Neuroimaging Initiative (ADNI)

Centre for Research on Ageing, Health and Wellbeing, The Australian National University, Canberra, Australia

Abstract: *Background:* While acceleration in age-related cerebral atrophy has been well documented in Alzheimer's disease, the cerebellar contributions to this effect have not been thoroughly investigated. Objective: This study investigated cerebellar volume and atrophy rate using magnetic resonance imaging in individuals with normal cognition (CN), mild cognitive impairment (MCI), and Alzheimer's disease (AD). Methods: Two hundred twenty-nine CN, 398 MCI and 191 AD participants of stage I ADNI database with screening scans were evaluated for cerebellar volume. Of those, 758 individuals with two or more follow-up scans were categorized into stable, converted, and reverted CN, MCI and AD and evaluated for cerebellar atrophy rate. Results: Cerebellar volume was 2.5% larger in CN than in those with AD but there were no differences between CN and MCI and MCI and AD in cross-sectional analysis. Similarly, the atrophy rate was 49% larger in AD and 64% larger in MCI who converted to AD but no difference was detected between CN and MCI. There were no association between education and APOEe4 and cerebellar volume or cerebellar atrophy across the diagnostic groups. Conclusion: Cerebellar atrophy contributes to Alzheimer's clinical progression but mostly at the late stage of the disease. However, even in the late stage shrinkage rate is less than the average of the shrinkage in the cerebrum and is not associated with AD moderators. This suggests that cerebellar involvement is secondary to cerebral involvement and can be due to network connection spread regardless of the primary pathology. *Hum Brain Mapp 38:3141–3150, 2017.* © 2017 Wiley Periodicals, Inc.

Key words: Alzheimer's disease; mild cognitive impairment; cerebellar atrophy; cerebellum; magnetic resonance imaging

Contract grant sponsor: Alzheimer's Disease Neuroimaging Initiative (ADNI) (National Institutes of Health Grant); Contract grant number: U01 AG024904; Contract grant sponsor: Department of Defense (DOD ADNI); Contract grant number: W81XWH-12-2-0012; Contract grant sponsor: National Institute on Aging, the National Institute of Biomedical Imaging and Bioengineering; Contract grant sponsor: Australian Research Council (to N.C.); Contract grant number: 120101705; Contract grant sponsor: Canadian Institutes of Health Research.

*Correspondence to: Hossein Tabatabaei-Jafari, Centre for Research on Ageing, Health and Wellbeing, Australian National University, Florey Building 54, Mills Road, Acton, ACT 2601, Australia.
E-mail: hossein.tabatabaei@anu.edu.au

Received for publication 19 November 2016; Revised 27 February 2017; Accepted 11 March 2017.

DOI: 10.1002/hbm.23580

Published online 21 March 2017 in Wiley Online Library (wileyonlinelibrary.com).

INTRODUCTION

The human cerebellum is a brain structure well known for its role in motor function and recently has drawn attention for its implication in cognitive functions [Schmahmann and Sherman, 1998; Stoodley, 2012; Weier et al., 2014; Wolf et al., 2009]. It is connected to almost all parts of the nervous system, comprises more than 50% of the total brain neurons, but surprisingly contributes to only 10% of the whole brain volume [Andersen et al., 1992]. This mismatch is a reflection of the difference in neural architecture. Gray matter makes up 80% of the cerebellar volume (compared with less than half for the cerebrum) [Hoogendam et al., 2012] and consists of densely packed small granular neurons tightly folded which are less diverse compared to those of the cerebral cortex. In contrast to the variety of cytoarchitectonic organisation observed in different regions of the cerebral cortex, all regions of the cerebellar cortex appear similar in histological sections [Standring, 2008]. Specific histological architecture in addition to rich connections to the other parts of the brain makes the cerebellum an important region to investigate in the context of neurodegenerative disorders.

Pathologically, Alzheimer's disease (AD) is characterized by abnormal intra and extra cellular protein aggregations, i.e., intracellular tau phosphorylation and extracellular β-amyloid deposition. Studies using positron emission tomography (PET) revealed significant correlations between postmortem and in vivo presence and density of amyloid plaques and phosphorylated tau: ^{11}C-labeled Pittsburgh compound B (^{11}C-PiB) [Driscoll et al., 2012] and Florbetapir-PET imaging [Clark et al., 2011] for β-amyloid deposition and labelled THK5117-PET [Lemoine et al., 2015] for aggregated hyperphosphorylated tau. PET studies suggested no difference in the cerebellar uptake in AD and cognitively normal (CN) participants [Jack et al., 2008b; Jonasson et al., 2016; Rowe et al., 2007] and therefore it has been adopted as a normalizing area for standardized uptake values (SUVs) [Jonasson et al., 2016; Lopresti et al., 2005].

Although AD related shrinkage and neuronal death are thought to be associated with and possibly due to β-amyloid deposition and tau aggregation [Wang et al., 2002], their topological patterns and progression are different [Braak and Braak, 1991; Thal et al., 2002]. Moreover, the pattern of regional brain atrophy in AD does not follow precisely either β-amyloid or tau topological patterns [Sluimer et al., 2009]. Therefore, normal level of β-amyloid deposition and tau aggregation may not rule out the presence of neuronal loss or shrinkage in the cerebellum. A recent postmortem stereological study suggested no significant differences in the cerebellar total Purkinje and granular cell number nor in the volume of the granular layer between severely demented Alzheimer's disease (AD) and normal individuals [Andersen et al., 2012]. However, this finding is inconsistent with a previous study that showed a significant reduction in the granular layer in AD [Wegiel et al., 1999] although both studies reported significant reduction in whole cerebellar volume. These somewhat inconsistent findings may be due to the fact that these studies were postmortem (cross-sectional) with low sample sizes (20 and 16 subjects, respectively) in qualitatively different cohorts and thus afforded low statistical power.

To bypass the inevitable limitations of post mortem studies (single measurement occasion and small sample size), structural neuroimaging techniques including magnetic imaging are the best available option for longitudinal examination of brain volume change over time. Our recent published systematic review [Tabatabaei-Jafari et al., 2015] revealed that there is no morphological longitudinal study aimed at comparing cerebellar structural change in normal ageing and cognitively impaired populations including mild cognitive impairment (MCI) and Alzheimer's disease. Therefore, the main aim of this study is to evaluate cross-sectional and longitudinal structural differences in the cerebellum across cognitively different populations including CN, MCI, and AD.

METHODOLOGY

Study Participants

Data used in the preparation of this article were obtained from the Alzheimer's Disease Neuroimaging Initiative (ADNI) database (adni.loni.usc.edu). The ADNI was launched in 2003 as a public–private partnership, led by Principal Investigator Michael W. Weiner, MD. The primary goal of ADNI has been to test whether serial magnetic resonance imaging (MRI), positron emission tomography (PET), other biological markers, and clinical and neuropsychological assessment can be combined to measure the progression of MCI and early AD.

All individuals participating in ADNI1 study who underwent MRI screening and diagnostic evaluations were included in the cross-sectional analysis and categorized into three diagnostic groups: CN, MCI, and AD. Participants with additional scans in follow-up assessments were included in the longitudinal analysis and categorised into more specific diagnostic groups according to the diagnosis at the first and last scanning time points. Details of the diagnostic criteria can be found on the ADNI web site (http://www.adni-info.org/Scientists/AboutADNI.aspx). Briefly, participants were categorized as CN if they had a Mini Mental State Examination (MMSE) score higher than 24, a Clinical Dementia Rating (CDR) of 0 and were not diagnosed with MCI, dementia or depression. Participants were categorized as MCI if they had a MMSE score higher than 24, a subjective report of memory concern, a measured objective memory loss, a CDR of 0.5, absence of dementia and preserved daily living activities. Participants were categorized as AD if they had a MMSE score lower than 26, a CDR of 0.5 or 1.0, and fulfilled criteria for clinically probable AD according to the Institute of Neurological and Communicative Diseases and Stroke/Alzheimer's Disease and Related Disorders Association. Participants with follow-up evaluation were categorized

into stable, converted or reverted CN, MCI, and AD according to the first and last time points diagnoses: stable if the first and last evaluation were similar, converted if the last evaluation progressed to declined cognitive diagnosis and reverted if the last evaluation was improved.

Image Acquisition

Participants underwent a high-resolution MRI scans of the brain on 1.5 T scanners from General Electric, Siemens, or Philips (Milwaukee, WI; Germany; The Netherlands, respectively) across multiple scanners using a standardized MRI protocol for 3D MP-RAGE sequences [Jack et al., 2008a] and following parameters: TR = 2,400 ms, minimum full TE, TI = 1,000 ms, flip angle = 8°, 24 cm field of view, acquisition matrix of 192 × 192 × 166 and yielding 1.25 × 1.25 × 1.2 mm^3.

Segmentation and Image Analysis

Volumetric segmentation were conducted by the ADNI team at the University of California, San Francisco using FreeSurfer version 5.1 for longitudinal analyses [Reutera et al., 2012]. The cerebellum was automatically segmented into gray matter and white matter. Sum values of the gray and white matter were considered as hemisphere volume and total of left and right were considered as cerebellar volumes.

Statistical Analysis

The R statistical software (version 3.1.1) was used for the cross-sectional and longitudinal analyses. The intra-class correlation coefficient (ICC) for the repeated longitudinal cerebellar volumes measurements was 0.98 (95%CI 0.9803–0.9843), which indicates that most of the variance (~96%) occurs between participants while only 4% occurs within participants.

Nonparametric locally weighted scatterplot smoothing (LOWESS) was used to visually inspect the data to determine whether linear models were appropriate. The LOWESS approach uses weighted least squares (giving more weight to points near the point whose response is being estimated) to estimate the mean response value at each time point and provide a smooth line representing the relationship between dependent and explanatory variables, when there are no assumptions about the relationship. The LOWESS plots for cerebellar volume versus age suggested that linear modeling of the relationship between cerebellar volume and age was appropriate for cross-sectional and longitudinal analyses since little departure from linearity was observed across groups except for CNc, which assumed to be due to low sample size i.e. 19 participants (Fig. 1).

The lme4 package (version 1.1-7) was used to conduct linear regressions analyses. In cross-sectional analyses, multiple linear regressions were conducted to investigate

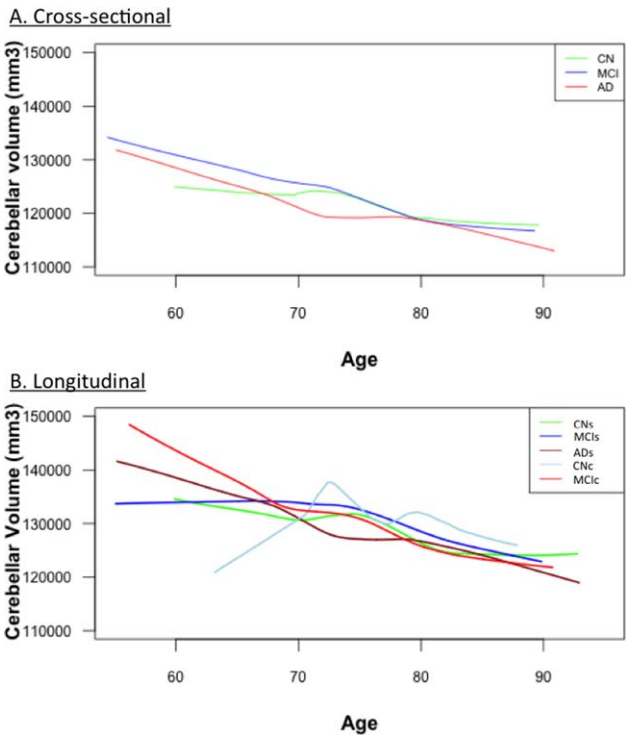

Figure 1.
Locally weighted smoothed mean measurement trajectory (LOWESS plot) of cerebellar volumes vs. age. (**A**) Three clinical groups including cognitively normal (CN), mild cognitive impairment (MCI), and Alzheimer's disease (AD) in cross-sectional level. (**B**) Five clinical groups including stable cognitively normal (CNs), cognitively normal converted to mild cognitive impairment (CNc), stable mild cognitive impairment (MCIs), mild cognitive impairment converted to AD (MCIc), and stable Alzheimer's disease (ADs) in serial scans. [Color figure can be viewed at wileyonlinelibrary.com]

the cross-sectional relationship between cerebellar volume and clinical diagnosis status. Cerebellar volume was applied as dependent variable and age (centred on 55, the youngest participants at baseline), gender, education, APOE e4, diagnosis and intracranial volume (ICV) were considered as explanatory variables. In longitudinal analyses, mixed effects models were applied with the same explanatory variables for linear regressions in addition to a random effect by scanner and two random effects by subjects: a random intercept and a random slope for age at each time point. The random slope of time (centred age at each time point) was tested in a minimally controlled model and if statistically significant was included in the model as random effect [Bernal-Rusiel et al., 2013]. A time by clinical diagnosis group interaction effect was tested to determine whether the rate of change in cerebellar volume differed between groups. Fixed effect of age on cerebellar volume for each diagnostic group was considered as cerebellar atrophy rate.

TABLE I. Demographic information

	Cross-sectional ($N = 818$)			Longitudinal ($N = 758$)						
	CN	MCI	AD	CNs	CNc	MCIs	MCIc	CN to AD	ADs	MCIr	ADr
No. participants	229	398	191	196	19	193	161	2	172	13	2
Age at baseline (yr) (SD)	75.87 (5.02)	74.74 (7.39)	75.27 (7.46)	75.76 (5.03)	77.45 (5.22)	75.00 (7.42)	74.73 (6.71)	80.55 (3.61)	75.12 (7.61)	73.43 (9.96)	79.50 (4.38)
Male sex, *n* (%)	119 (52)	257 (65)	100 (52)	103 (53)	11 (58)	124 (64)	101 (63)	0 (0)	91 (53)	9 (69)	2 (100)
Education (yr) (SD)	16.07 (2.86)	15.64 (3.03)	14.70 (3.15)	16.13 (2.88)	15.95 (2.39)	15.45 (3.15)	15.84 (2.81)	15.00 (0.00)	14.77 (3.14)	16.00 (2.42)	16.00 (0.00)
APOEe4 (*n*) (%)	61 (27)	212 (53)	127 (67)	49 (25)	8 (42)	92 (48)	104 (65)	1 (50)	117 (68)	4 (31)	1 (50)
MMSE at baseline (SD)	29.11 (0.99)	27.03 (1.78)	23.31 (2.04)	29.08 (1.06)	29.32 (0.75)	27.22 (1.77)	26.71 (1.72)	29.5 (0.71)	23.40 (1.97)	27.85 (1.77)	26.00 (0.00)

CN, cognitively normal; MCI, mild cognitive impairment; AD, Alzheimer's disease; CNs, stable cognitively normal, cognitively normal converted to mild cognitive impairment; MCIs, stable mild cognitive impairment; MCIc, mild cognitive impairment converted to Alzheimer's disease; Ads, stable Alzheimer's disease; MCIr, mild cognitive impairment reverted to cognitively normal; ADr, Alzheimer's disease reverted to mild cognitive impairment; APOEe4, Apolipoprotein alleles e4 genotype; MMSE, mini-mental state examination.

The final models were visually checked for any obvious deviations from homoscedasticity, normality of residuals, and linearity. Likelihood ratio test of the model with the effect in question against the model without was used to determine statistical significance.

RESULTS

Demography

Cross-sectional

Eight hundred eighteen participants were categorized into CN, MCI, and AD. There were no significant differences in age across the groups, but significant differences in gender and APOE e4 distributions among the diagnostic groups. The male ratio was higher in MCI and, as expected, APOEe4 frequencies were significantly higher in MCI and AD. AD participants were significantly less educated than CN (Table I).

Longitudinal

Of 818 participants with screening scans 758, who had one or more follow-up scans and cognitive tests, were included in the longitudinal part. They were categorized into different diagnostic groups according to the first and last time points diagnoses: stable CN (CNs), CN converted to MCI (CNc), stable MCI (MCIs), MCI converted to AD (MCIc), stable AD (ADs), CN converted to AD, MCI reverted to CN (MCIr), and AD reverted to MCI (ADr). There were no significant differences in age and education across the diagnostic groups except for education between CNs and ADs. Pearson χ^2 test revealed no significant difference in gender distribution but a significant difference in APOEe4 distributions between diagnostic groups. APOEe4 distributions were higher in MCIs than CNs and in ADs than CNs. The mean follow-up period across the groups was 2.54 (1.20) years, which was shorter in MCIs and ADs compared with CNs.

Cross-Sectional Results

A significant association between cognitive diagnosis and cerebellar volume ($F_{(2,811)} = 3.95$, $P < 0.01$) was detected.

Pairwise comparisons demonstrated (3,400 mm^3; ~2.5%) larger cerebellar volume in CN compared to AD ($F_{(1,413)} = 9.82$, $P < 0.001$), but no differences between CN and MCI ($F_{(1,620)} = 3.40$ $P > 0.1$), and MCI and AD ($F_{(1,582)} = 1.62$, $P > 0.1$). Table II presents the mean ICV-adjusted cerebellar volumes and the fixed effect of age for the three diagnostic groups. Although, the average cerebellar volume was significantly smaller in AD compared to CN and MCI, the slope of decrease in cerebellar volume for each year increase in age was only 0.41% (CN; 0.34%, MCI; 0.42%, AD; 0.38%) and was not significantly different across groups ($F_{(2,809)} = 0.28$, $P > 0.5$) and in pair-wise comparisons ($F < 0.5$, $P > 0.1$). When all explanatory variables were included, the linear regression

TABLE II. Cerebellar measures

	Cross-sectional ($N = 818$)			Longitudinal ($N = 758$)							
	CN	MCI	AD	CNs	CNc	MCIs	MCIc	CN to AD	ADs	MCIr	ADr
No. participants	229	398	191	196	19	193	161	2	172	13	2
Baseline volume (mm^3) (SD)[a]											
Total	123,249.80	122,394.90	120,706.90	131,276.60	132,820.00	130,319.50	130,154.90	131,354.80	129,524.10	131,603.50	114,157.80
	(10,018.69)	(10,632.40)	(10,591.60)	(11,163.98)	(9,450.25)	(11,317.70)	(11,680.98)	(778.99)	(10,838.42)	(10,703.89)	(17,439.08)
Left	61,739.12	60,420.98	60,193.35	65,382.32	66,270.67	64,842.59	64,934.41	63,636.93	64,600.50	65,556.00	57,525.16
	(6,539.80)	(6,431.27)	(7,254.14)	(5,724.23)	(4,846.23)	(5,688.15)	(5,939.78)	(154.53)	(5,454.41)	(5,127.40)	(9,387.68)
Right	62,498.44	61,213.30	60,910.64	65,894.26	66,549.30	65,476.95	65,220.46	65,717.89	64,923.62	66,047.48	56,632.64
	(6,404.02)	(6,584.98)	(7,329.76)	(5,570.00)	(4,843.58)	(5,784.85)	(5,943.95)	(624.47)	(5,525.67)	(5,681.92)	(8,051.40)
Follow-up period (yr) (SD)	—	—	—	3.12	3.52	2.41	2.84	2.99	1.61	2.68	3.45
				(1.18)	(0.73)	(1.24)	(1.08)	(0.00)	(0.62)	(1.09)	(0.76)
No. scan	1	1	1	4.81	5.21	4.76	5.38	5.00	3.48	4.31	4.00
				(1.15)	(0.86)	(1.57)	(1.37)	(0.00)	(0.38)	(1.44)	(0.00)
Last scan volume (mm^3) (SD)[b]											
Total	—	—	—	129,686.50	130,245.70	129,016.00	127,633.00	130,699.20	128,100.80	131,491.30	118,023.80
				(11,392.32)	(9,597.18)	(11,286.36)	(11,669.41)	(3,139.66)	(10,866.31)	(10,366.15)	(7,945.15)
Left	—	—	—	64,607.51	64,839.90	64,181.13	63,673.82	65,943.72	63,894.04	65,287.25	59,466.88
				(5,804.00)	(5,017.74)	(5,647.45)	(5,896.68)	(1,230.14)	(5,467.48)	(5,149.04)	(4,355.83)
Right	—	—	—	65,078.97	65,405.81	64,834.86	63,959.14	64,755.50	64,206.73	66,204.10	58,556.96
				(5,704.68)	(4,766.31)	(5,813.87)	(5,960.80)	(1,909.52)	(5,560.26)	(5,307.67)	(3,589.32)
Coef. of age (CS)/atrophy rate (longi)[c] (mm^3/yr) (SE)											
Total	−417.90	−531.60	−463.50	511.98	615.84	498.71	833.04	—[d]	747.84	373.60	—§
	(128.80)	(70.33)	(100.70)	(53.27)	(120.36)	(68.52)	(79.52)		(80.79)	(201.40)	
Left	−192.90	−256.30	−238.30	249.79	347.77	249.66	412.00	—	362.69	153.72	
	(66.25)	(35.39)	(50.17)	(28.39)	(62.36)	(37.03)	(41.59)		(41.92)	(83.20)	
Right	−225.00	−275.30	−225.30	262.54	271.53	248.74	419.13	—	374.76	200.00	
	(64.35)	(36.09)	(51.90)	(26.66)	(66.57)	(33.28)	(39.83)		(40.90)	(95.16)	

[a]The mean of cerebellar volume adjusted by the intra cranial volume for the cross-sectional part and baseline volume adjusted by the intra cranial volume for the longitudinal part.
[b]Adjusted by the intra cranial volume.
[c]Fixed effects of age for the cross-sectional data; extracted from the linear regression adjusted by intra cranial volume, gender, education and APOEe4, and atrophy rate for the longitudinal data; extracted from the linear mixed effects model adjusted by intra cranial volume, gender, education and APOEe4.
[d]Insufficient data for calculation.
CN, cognitively normal; MCI, mild cognitive impairment; AD, Alzheimer's disease; CNs, stable cognitively normal; cognitively normal converted to mild cognitive impairment; MCIs, stable mild cognitive impairment; MCIc, mild cognitive impairment converted to Alzheimer's disease; Ads, stable Alzheimer's disease; MCIr, mild cognitive impairment reverted to cognitively normal; ADr, Alzheimer's disease reverted to mild cognitive impairment; APOEe4, Apo lipoprotein alleles e4 genotype; MMSE; mini-mental state examination.

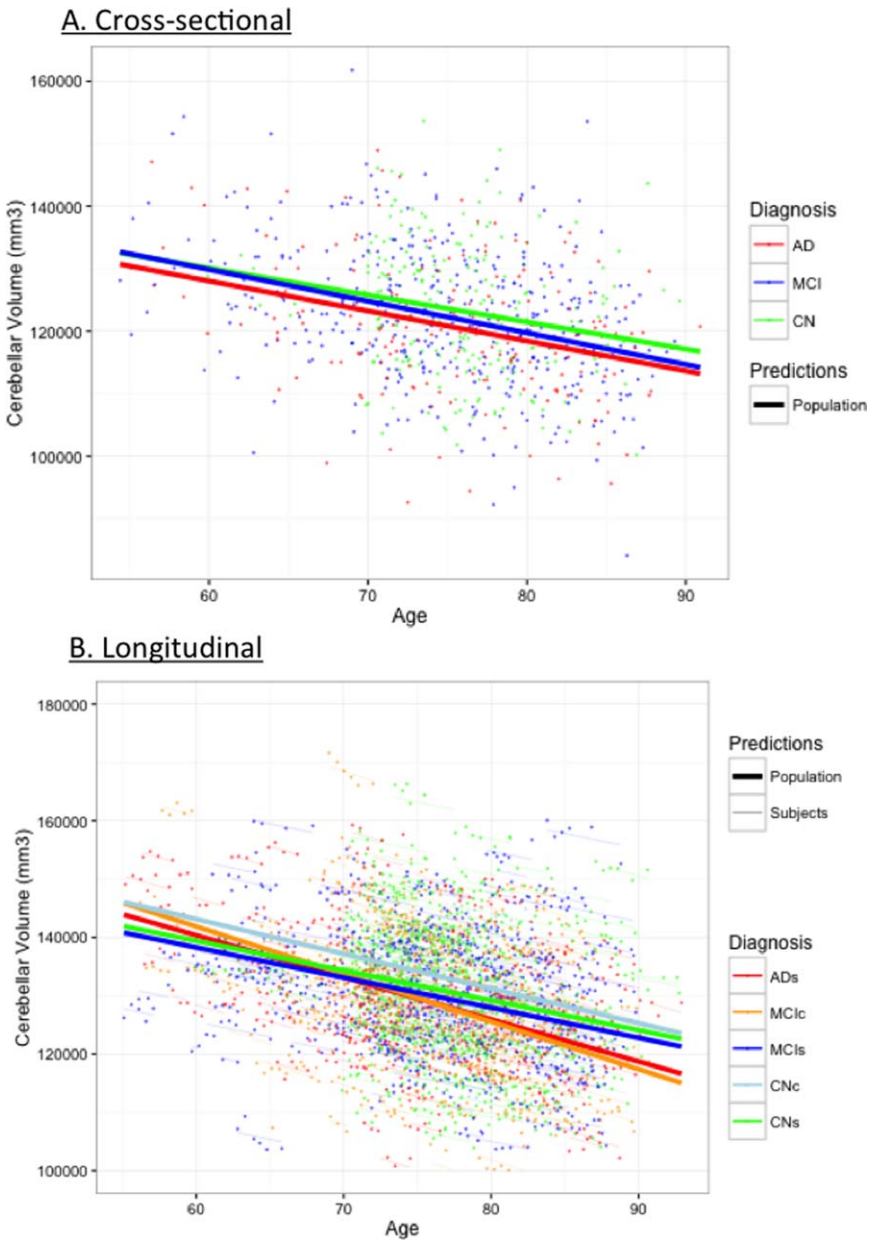

Figure 2.

Linear prediction of the cerebellar volumes for age at time points. (**A**) Prediction of the cerebellar volumes in three clinical groups including cognitively normal (CN), mild cognitive impairment (MCI) and Alzheimer's disease (AD) in cross-sectional level. (**B**) Prediction in subject and group (population) levels in five diagnostic groups including stable cognitively normal (CNs), cognitively normal converted to mild cognitive impairment (CNc), stable mild cognitive impairment (MCIs), and mild cognitive impairment converted to AD (MCIc) illustrating different slops for the diagnostic groups. [Color figure can be viewed at wileyonlinelibrary.com]

model explained 44.7% of the variance in cerebellar volume ($F_{(8,809)} = 83.61$, $P < 0.0001$) mostly explained by ICV (37.9%) with 7.7% explained by age alone, and 0.7% by clinical group.

The scatters plot presenting the association between age and cerebellar volume for each group also revealed an initial overlap of CN and MCI regression lines followed by deviation of MCI regression line to AD line suggesting that cerebellar volumes are highly similar in CN and MCI at younger ages but lower in MCI in older individuals (Fig. 2A). In contrast the AD regression line while following a similar

TABLE III. Pair-wise comparison of group diagnosis

	CNs vs. CNc		CNs vs. MCIs		CNs vs. MCIc		CNs vs. ADs	
	Model 1	Model 2	Model 1	Model 2	Model 1	Model 2	Model 1	Model 2
Intercept	142,212.26	146,127.2	139,769.58	139,091.58	137,510.50	139,282.56	138,821.74	141,244.50
	(4,460.56)	(6,078.7)	(3,247.02)	(3,445.00)	(3,521.38)	(3,755.78)	(3,172.06)	(3,523.62)
Volume slope in CNs (mm^3/yr) (SE)	—	−4,286.9	—	1,745.53	—	−3,236.69	—	−1,504.24
		(4,450.6)		(2,164.33)		(2,257.59)		(2,371.78)
Pr(>|t|)	—	0.3366[a]	—	0.421[a]	—	0.1525[a]	—	0.5263[a]
Shrinkage slope in CNs (mm^3/yr) (SE)	—	100.9	—	−19.72	—	312.57	—	214.37
		(163.6)		(84.54)		(91.80)		(94.66)
Pr(>|t|)	—	0.5382[a]	—	0.816[a]	—	**0.0007**[d]	—	**0.0240**[b]
Loglik	−9,793	−9,793	−1,7438	−1,7438	−1,6960	−1,6951	−14,515	−14,509
Chisq						17.126		10.884
Chi *df*		1.0195		1.3075		2		2
		2		2				
Pr (>Chisq)		0.6006[a]		0.5201[a]		**0.0001911**[d]		**0.004332**[c]

[a]Significant code: >0.1.
[b]Significant code: <0.01.
[c]Significant code: <0.001.
[d]Significant code: <0.0001.
CN, cognitively normal; CNs, stable cognitively normal; CNc, cognitively normal converted to mild cognitive impairment; MCIs, stable mild cognitive impairment; MCIc, mild cognitive impairment converted to Alzheimer's disease; ADs, stable Alzheimer's disease.

slope had a clearly different intercept suggesting a constant smaller cerebellar volume in AD across the age span investigated. Similar patterns were demonstrated for the left and right cerebellar volumes (Table II).

Longitudinal Results

The linear mixed model achieved a good fit and fixed factors in the model explained 43% (marginal R^2) while fixed and random factors together explained 99% (conditional R^2) of variance in cerebellar atrophy. A significant negative fixed effect of age was detected ($\chi^2_{(1,9)} = 586.99$, $P < 0.0001$); each year beyond age 55 was associated with a 0.47% lower cerebellar volume compared to baseline. Additionally, a significant random effect of age on cerebellar volume ($\chi^2_{(2,18)} = 227.92$, $P < 0.0001$) and interaction between age and diagnosis ($\chi^2_{(7,25)} = 22.72$, $P < 0.01$) were detected. The model revealed no differences in cerebellar volume across the diagnostic groups ($\chi^2_{(7,18)} = 11.31$, $P > 0.1$), i.e., the average of cerebellar volumes in CNs, CNc, MCIs, MCIc, and ADs were not significantly different. However, a significant effect of cognitive diagnosis on cerebellar atrophy rates was detected ($\chi^2_{(7,25)} = 22.71$, $P < 0.001$). There was also a significant effect of gender on cerebellar volume (1,18) = 14.12, $P < 0.001$) with less shrinkage in male.

An annual shrinkage of 0.36% (SE = 0.04) was detected in CNs individuals. A pairwise comparison revealed that it was not significantly different in MCIs (0.36%/year, SE = 0.05) and CNc (0.42%/year, SE = 0.08); however, it was about 49% larger in ADs (0.53%/year, SE = 0.06). Similarly, the atrophy rate was about 64% larger in MCIc (0.62%/year, SE = 0.06) compared to CNs (Tables II and III). The annual atrophy was also about 53% larger in ADs than MCIs ($\chi^2_{(2,13)} = 8.67$ $P < 0.01$) and 68% larger in MCIc than MCIs ($\chi^2_{(2,13)} = 12.57$, $P < 0.001$; Table II). CN who converted to AD, MCI who reverted to CN and AD who reverted to MCI were excluded from pairwise comparison due to small samples sizes. Atrophy trajectories across groups are presented in Figure 2B.

Similar patterns of findings were observed for the left and right cerebellar volumes (Table II), as well as left and right cerebellar gray matter and white matter volumes.

DISCUSSION

This study aimed to investigate cerebellar shrinkage in normal ageing and preclinical (MCI) and clinical phases of AD. It revealed that cerebellar shrinkage occurs mostly in the late stages of the disease. The main findings were that (1) in cross-sectional analyses cerebellar volume was larger in CN compared to AD but not compared to MCI, (2) in longitudinal analyses cerebellar atrophy was higher in ADs and MCIc compared to CNs but not in CNc and MCIs, and (3) APOEe4 was not a significant predictor of baseline cerebellar volume nor of cerebellar atrophy across clinical groups.

Cross-Sectional

The smaller cerebellar volume observed in AD compared to CN and no difference between MCI and CN are in agreement with available cross-sectional studies reporting smaller cerebellar volume in AD [Kusbeci et al., 2009; Moller et al., 2013] but normal volume in MCI [Thomann et al., 2008; Yoon et al., 2013]. This discrepancy is consistent with the documented progression of AD pathology. However, the cerebellum can be parsed functionally and morphologically into different subdivisions and it is likely that AD pathology targets each subdivision differently. Previous voxel-based morphometric studies showed bilateral lower gray matter density in lobule VI [Colloby et al., 2014] and Crus I/II [Guo et al., 2016] in AD compared with CN, suggesting that network-selective vulnerability underlies the cerebellar neurodegeneration [Guo et al., 2016]. Regardless of selective or nonselective volume loss in the cerebellum and its subregions, cross-sectional approach needs to be affirmed by tracking atrophy in a longitudinal approach.

Longitudinal

The negative association between age and cerebellar volume is consistent with that demonstrated in the cross-sectional analysis (0.41%/year in cross-sectional and 0.47% in longitudinal). Pairwise analyses demonstrated significantly larger cerebellar atrophy rates in ADs and MCIc but not in CNc and MCIs compared to CNs. This pattern of results is suggestive of an increasing rate of cerebellar atrophy with progression of AD pathology. It is also consistent with the chronological development of AD pathology with progressive spreading of tau fibrillatory tangles (Braak stages), amyloid deposition, and subsequently gradual decline in cognitive function [Murray et al., 2015]. As Thal et al. demonstrated, clinically diagnosed AD occurs in the amyloid phase 3 to 5 while the cerebellar involvement mostly occurs in the fifth phase [Thal et al., 2002]. Thus, the available evidence suggests that the cerebellum is relatively spared of neurodegeneration in the preclinical stages of the disease and gradually becomes affected as the clinical presentation fully develops. However, it remains unclear whether association of the cerebellum with AD clinical progression is due to spreading of fibrillary tangle and/or amyloid deposition, or secondary to cerebral neurodegeneration.

Although the findings suggest shrinkage in the cerebellum with ageing and larger cerebellar atrophy in ADs compared with CNs and MCIs, it is worthy to consider that cerebellar atrophy in the diagnostic groups were less than that reported for whole brain atrophy (CNs: 0.36%/year versus 0.57%/year; MCIs: 0.36%/year versus 1.02%/year; ADs: 0.53%/year versus 1.90%/year) [Henneman et al., 2009; Tabatabaei-Jafari et al., 2015]. This is in contrast to brain areas characteristics for AD pathology, including hippocampus and entorhinal cortex, for which atrophy rates are roughly 200% higher for MCI and 300% higher for AD compared to normal ageing [Desikan et al., 2008; Tabatabaei-Jafari et al., 2015], further emphasising the relative resistance of the cerebellum to AD related degeneration. However, despite the small effect size and partial resistance, the cerebellum is not intact in AD pathology and future investigation is needed to elucidate the impact of cerebellar atrophy on uptake measurement when using the cerebellum to standardise FDG uptake in PET studies.

Covariates and Correlates

Age is a common predictor for CN and AD-related brain atrophy and all cognitive groups in the current study were matched for age. However, they were differences in gender distribution, education and APOEe4 alleles—the most well-known risk factors of AD pathology—as were expected. An effect of sex on cerebellar volume was detected such that males showed less cerebellar atrophy than females. However, no significant association between education or APOEe4 alleles and cerebellar volume were detected. APOEe4 is a known moderator of hippocampal atrophy in AD pathology [Tabatabaei-Jafari et al., 2015], therefore it might have been expected that carrying the APOEe4 allele would be associated with increased cerebellar atrophy. However, this was not the case in our findings. It may indicate that while neurodegeneration in the cerebrum is directly related to the development of neurofibrillary tangles and β-amyloid deposition which occurs at higher rates in APOEe4 carriers, cerebellar atrophy is the product of secondary processes associated with cerebral neuronal loss, Wallerian degeneration, and widespread disconnection. To clarify this question future investigations need to further elucidate the impact of risk factors in different AD clinical stages.

Strengths and Limitation

This study is unique in using in vivo evaluation of the cerebellum with a reasonable follow up period in a relatively large sample while computing both cross-sectional and longitudinal estimates and using advanced and well-controlled mixed-effects models. Most AD related cerebellar studies conducted to date have been postmortem or if in vivo, cross-sectional in design, thus raising questions as to the precision and generalizability of their estimates. Consequently, the present study fills an important gap. However, it should be noted that this investigation was restricted to the gray and white matter volumes in the left and right cerebellum and therefore do not provide information on the cerebellar subregions.

CONCLUSION

The cerebellum is often thought to be spared from neurodegenerative processes but the present findings indicate that this is not the case. The present findings demonstrate that although the cerebellum is not significantly affected in

the preclinical phase of AD (i.e. MCI), it is affected in the clinical phase. However, acceleration in atrophy rate is less than the average of the atrophy in the cerebrum and it is not associated with AD moderators (education and APOEe4 status). These findings in addition to previous evidence of network-selective vulnerability of the cerebellum suggest that AD-related cerebellar atrophy might be secondary to the development of AD pathology in the cerebrum rather than the cerebellum itself. Therefore, modifying interventions targeting the non-specific network progression is a potential therapeutic option additional to interventions targeting the specific pathological process.

ACKNOWLEDGMENTS

Data used in preparation of this article were obtained from the Alzheimer's Disease Neuroimaging Initiative (ADNI) database (adni.loni.usc.edu). As such, the investigators within the ADNI contributed to the design and implementation of ADNI and/or provided data but did not participate in analysis or writing of this report. A complete listing of ADNI investigators can be found at http://adni.loni.usc.edu/wp-content/uploads/how_to_apply/ADNI_Acknowledgement_List.pdf. H.T.J.: study concept, design, data management, statistical analyses, and managed all aspects of manuscript preparation and submission. E.W.: statistical analysis, and manuscript preparation. M.E.S.: image analysis, and manuscript preparation. N.C.: study design, methodological input and theoretical expertise, and manuscript preparation. ADNI is funded by the National Institute on Aging, the National Institute of Biomedical Imaging and Bioengineering, and through generous contributions from the following: AbbVie, Alzheimer's Association; Alzheimer's Drug Discovery Foundation; Araclon Biotech; BioClinica, Inc.; Biogen; Bristol-Myers Squibb Company; CereSpir, Inc.; Cogstate; Eisai Inc.; Elan Pharmaceuticals, Inc.; Eli Lilly and Company; EuroImmun; F. Hoffmann-La Roche Ltd. and its affiliated company Genentech, Inc.; Fujirebio; GE Healthcare; IXICO Ltd.; Janssen Alzheimer Immunotherapy Research & Development, LLC.; Johnson & Johnson Pharmaceutical Research & Development LLC.; Lumosity; Lundbeck; Merck & Co., Inc.; Meso Scale Diagnostics, LLC.; NeuroRx Research; Neurotrack Technologies; Novartis Pharmaceuticals Corporation; Pfizer Inc.; Piramal Imaging; Servier; Takeda Pharmaceutical Company; and Transition Therapeutics. The Canadian Institutes of Health Research is providing funds to support ADNI clinical sites in Canada. Private sector contributions are facilitated by the Foundation for the National Institutes of Health (www.fnih.org). The grantee organization is the Northern California Institute for Research and Education, and the study is coordinated by the Alzheimer's Therapeutic Research Institute at the University of Southern California. ADNI data are disseminated by the Laboratory for Neuro Imaging at the University of Southern California.

REFERENCES

Andersen BB, Korbo L, Pakkenberg B (1992): A quantitative study of the human cerebellum with unbiased stereological techniques. J Comp Neurol 326:549–560.

Andersen K, Andersen BB, Pakkenberg B (2012): Stereological quantification of the cerebellum in patients with Alzheimer's disease. Neurobiol Aging 33:197.e11–197.e120.

Bernal-Rusiel JL, Greve DN, Reuter M, Fischl B, Sabuncu MR, Initiative ADNI. (2013): Statistical analysis of longitudinal neuroimage data with linear mixed effects models. Neuroimage 1: 249–260.

Braak H, Braak E (1991): Neuropathological stageing of Alzheimer-related changes. Acta Neuropathol. 82:239–259.

Clark CM, Schneider JA, Bedell BJ, Beach TG, Bilker WB, Mintun MA, Pontecorvo MJ, Hefti F, Carpenter AP, Flitter ML, Krautkramer MJ, Kung HF, Coleman RE, Doraiswamy PM, Fleisher AS, Sabbagh MN, Sadowsky CH, Reiman EP, Zehntner SP, Skovronsky DM (2011): Use of florbetapir-PET for imaging beta-amyloid pathology. JAMA 305:275–283.

Colloby SJ, O'Brien JT, Taylor JP (2014): Patterns of cerebellar volume loss in dementia with Lewy bodies and Alzheimers disease: A VBM-DARTEL study. Psychiatry Res 223:187–191.

Desikan RS, Fischl B, Cabral HJ, Kemper TL, Guttmann CR, Blacker D, Hyman BT, Albert MS, Killiany RJ (2008): MRI measures of temporoparietal regions show differential rates of atrophy during prodromal AD. Neurology 71:819–825.

Driscoll I, Troncoso JC, Rudow G, Sojkova J, Pletnikova O, Zhou Y, Kraut MA, Ferrucci L, Mathis CA, Klunk WE, O'Brien RJ, Davatzikos C, Wong DF, Resnick SM (2012): Correspondence between in vivo (11)C-PiB-PET amyloid imaging and postmortem, region-matched assessment of plaques. Acta Neuropathol 124:823–831.

Guo CC, Tan R, Hodges JR, Hu X, Sami S, Hornberger M (2016): Network-selective vulnerability of the human cerebellum to Alzheimer's disease and frontotemporal dementia. Brain 139: 1527–1538.

Henneman WJ, Sluimer JD, Barnes J, van der Flier WM, Sluimer IC, Fox NC, Scheltens P, Vrenken H, Barkhof F (2009): Hippocampal atrophy rates in Alzheimer disease: Added value over whole brain volume measures. Neurology 72:999–1007.

Hoogendam YY, Geest JNvd, Lijn Fvd, Lugt Avd, Niessen WJ, Krestin GP, Hofman A, Vernooij MW, Breteler MMB, Ikram MA (2012): Determinants of cerebellar and cerebral volume in the general elderly population. Neurobiol Aging 33:2774–2781.

Jack CR Jr, Bernstein MA, Fox NC, Thompson P, Alexander G, Harvey D, Borowski B, Britson PJ, J LW, Ward C, Dale AM, Felmlee JP, Gunter JL, Hill DL, Killiany R, Schuff N, Fox-Bosetti S, Lin C, Studholme C, DeCarli CS, Krueger G, Ward HA, Metzger GJ, Scott KT, Mallozzi R, Blezek D, Levy J, Debbins JP, Fleisher AS, Albert M, Green R, Bartzokis G, Glover G, Mugler J, Weiner MW (2008a): The Alzheimer's Disease Neuroimaging Initiative (ADNI): MRI methods. J Magn Reson Imaging 27:685–691.

Jack CR Jr, Lowe VJ, Senjem ML, Weigand SD, Kemp BJ, Shiung MM, Knopman DS, Boeve BF, Klunk WE, Mathis CA, Petersen RC (2008b): 11C PiB and structural MRI provide complementary information in imaging of Alzheimer's disease and amnestic mild cognitive impairment. Brain 131:665–680.

Jonasson M, Wall A, Chiotis K, Saint-Aubert L, Wilking H, Sprycha M, Borg B, Thibblin A, Eriksson JP, Sorensen J, Antoni G, Nordberg A, Lubberink M (2016): Tracer kinetic

analysis of (S)-18F-THK5117 as a PET tracer for assessing tau pathology. J Nucl Med 57:574–581.

Kusbeci OY, Bas O, Gocmen-Mas N, Karabekir HS, Yucel A, Ertekin T, Yazici AC (2009): Evaluation of cerebellar asymmetry in Alzheimer's disease: A stereological study. Dementia Geriatr Cognit Disord 28:1–5.

Lemoine L, Saint-Aubert L, Marutle A, Antoni G, Eriksson JP, Ghetti B, Okamura N, Nennesmo I, Gillberg PG, Nordberg A (2015): Visualization of regional tau deposits using (3)H-THK5117 in Alzheimer brain tissue. Acta Neuropathol Commun 3:40.

Lopresti BJ, Klunk WE, Mathis CA, Hoge JA, Ziolko SK, Lu X, Meltzer CC, Schimmel K, Tsopelas ND, DeKosky ST, Price JC (2005): Simplified quantification of Pittsburgh compound B amyloid imaging PET studies: A comparative analysis. J Nucl Med 46:1959–1972.

Moller C, Vrenken H, Jiskoot L, Versteeg A, Barkhof F, Scheltens P, van der Flier WM (2013): Different patterns of gray matter atrophy in early- and late-onset Alzheimer's disease. Neurobiol Aging 34:2014–2022.

Murray ME, Lowe VJ, Graff-Radford NR, Liesinger AM, Cannon A, Przybelski SA, Rawal B, Parisi JE, Petersen RC, Kantarci K, Ross OA, Duara R, Knopman DS, Jack CR Jr, Dickson DW (2015): Clinicopathologic and 11C-Pittsburgh compound B implications of Thal amyloid phase across the Alzheimer's disease spectrum. Brain 138:1370–1381.

Reutera, M., Schmansky, N.J., Rosasa, D., Fischl, B. (2012) Within-subject template estimation for unbiased longitudinal image analysis. Neuroimage, 61:1402–1418.

Rowe CC, Ng S, Ackermann U, Gong SJ, Pike K, Savage G, Cowie TF, Dickinson KL, Maruff P, Darby D, Smith C, Woodward M, Merory J, Tochon-Danguy H, O'Keefe G, Klunk WE, Mathis CA, Price JC, Masters CL, Villemagne VL (2007): Imaging beta-amyloid burden in aging and dementia. Neurology 68:1718–1725.

Schmahmann JD, Sherman JC (1998): The cerebellar cognitive affective syndrome. Brain 121:561–579.

Sluimer JD, van der Flier WM, Karas GB, van Schijndel R, Barnes J, Boyes RG, Cover KS, Olabarriaga SD, Fox NC, Scheltens P, Vrenken H, Barkhof F (2009): Accelerating regional atrophy rates in the progression from normal aging to Alzheimer's disease. Eur Radiol 19:2826–2833.

Standring S. (2008): Gray's Anatomy. The Anatomical Basis of Clinical Practice, 40th ed. Churchill Livingstone, London.

Stoodley CJ (2012): The cerebellum and cognition: Evidence from functional imaging studies. Cerebellum (London, England) 11: 352–365.

Tabatabaei-Jafari H, Shaw ME, Cherbuin N (2015): Cerebral atrophy in mild cognitive impairment: A systematic review with meta-analysis. Alzheimer's Dementia 1:487–504.

Thal DR, Rub U, Orantes M, Braak H (2002): Phases of A beta-deposition in the human brain and its relevance for the development of AD. Neurology 58:1791–1800.

Thomann PA, Schlafer C, Seidl U, Santos VD, Essig M, Schroder J (2008): The cerebellum in mild cognitive impairment and Alzheimer's disease - A structural MRI study. J Psychiatr Res 42: 1198–1202.

Wang H-Y, D'Andrea MR, Nagele RG (2002): Cerebellar diffuse amyloid plaques are derived from dendritic A-beta 42 accumulations in Purkinje cells. Neurobiol Aging 23:213–223.

Wegiel J, Wisniewski HM, Dziewiatkowski J, Badmajew E, Tarnawski M, Reisberg B, Mlodzik B, De Leon MJ, Miller DC (1999): Cerebellar atrophy in Alzheimer's disease-clinicopathological correlations. Brain Res 818:41–50.

Weier K, Penner IK, Magon S, Amann M, Naegelin Y, Andelova M, Derfuss T, Stippich C, Radue E-W, Kappos L, Sprenger T (2014): Cerebellar abnormalities contribute to disability including cognitive impairment in multiple sclerosis. PLoS One 9: e86916.

Wolf U, Rapoport MJ, Schweizer TA (2009): Evaluating the affective component of the cerebellar cognitive affective syndrome. J Neuropsychiatry Clin Neurosci 21:245–253.

Yoon CW, Seo SW, Park JS, Kwak KC, Yoon U, Suh MK, Kim GH, Shin JS, Kim CH, Noh Y, Cho H, Kim MJ, Kim JH, Roh JH, Lee JM, Na DL (2013): Cerebellar atrophy in patients with subcortical-type vascular cognitive impairment. Cerebellum (London, England) 12:35–42.